Research Square

Preprints are preliminary reports that have not undergone peer review.
They should not be considered conclusive, used to inform clinical practice,
or referenced by the media as validated information.

Neuroimaging findings in hyperammonemic encephalopathy associated with sepsis-induced acute liver dysfunction: a pilot case series

Rustam Talybov

rustam230789@gmail.com

Tyumen State Medical University

Tatyana Trofimova

First Pavlov State Medical University of St. Petersburg

Tatyana Kleshchevnikova

Regional clinical hospital №2, Tyumen

Yauhen Statsenko

College of Medicine and Health Sciences, United Arab Emirates University

Research Article

Keywords: sepsis, acute liver dysfunction, hyperammonemia, hyperammonemic encephalopathy, MRI, case series

Posted Date: August 3rd, 2026

DOI: https://doi.org/10.21203/rs.3.rs-10420436/v1

License: This work is licensed under a Creative Commons Attribution 4.0 International License. Read Full License

Additional Declarations: No competing interests reported.

Version of Record: A version of this preprint was published at Neuroradiology on October 17th, 2026. See the published version at https://doi.org/10.1007/s00234-026-04230-2.

Abstract

Background. Hyperammonemic encephalopathy (HE) is a severe complication of acute liver dysfunction (ALD), often associated with sepsis. However, its neuroimaging manifestations remain poorly understood. The aim of this pilot case series is to describe the brain MRI findings in patients with sepsis and HE.
Methods. We analysed brain MRI data from 15 consecutive patients with sepsis and clinically confirmed HE. Assessment of cerebral changes was performed using a standard MRI protocol. The following parameters were evaluated during the analysis: localization and signal intensity characteristics of the lesions on MRI, presence or absence of diffusion restriction, presence magnetic susceptibility artifacts, and reversibility on follow-up were evaluated descriptively. No control group was included.
Results. Pathological changes were observed in all 15 patients. Symmetrical involvement of the insular cortex and cingulate gyrus was the most frequent pattern (13/15, 86.7%), followed by basal ganglia lesions (1/15) and cortico-subcortical hemispheric lesions (1/15). All lesions were hyperintense on T2-WI and FLAIR, with diffusion restriction on DWI suggestive of cytotoxic oedema. Follow-up MRI was performed in all patients after treatment adjustment and renal replacement therapy, demonstrating marked regression of all noted changes, concurrent with normalization of serum ammonia, transaminases, lactate and sepsis markers.
Conclusion. The bilateral insular-cingulate pattern appears to be the most common MRI finding in sepsis-related HE and shows reversibility upon correction of hyperammonaemia. These observations suggest that MRI may provide supportive evidence for early diagnosis, but the findings are preliminary and require validation in larger controlled studies.

Background

Sepsis is a life-threatening condition based on the dysregulation of the host's systemic response to an infectious agent, leading to the development of multiple organ failure [1]. Sepsis occupies one of the leading positions in the global mortality structure [2]. A significant proportion of sepsis survivors subsequently develop persistent impairments in physical, psychological, and cognitive status, which imposes a substantial burden on the healthcare [3–5]. The central pathogenetic element of sepsis is organ dysfunction, defined as the partial or complete loss of functional activity of the affected organ or organ system [4]. The spectrum of such disorders encompasses the cardiovascular, respiratory, hepatobiliary, urinary, and central nervous systems [5]. Among all forms of organ dysfunction in sepsis, acute liver dysfunction (ALD) occupies a dominant position and is identified in approximately 46% of patients. Mortality associated with this complication can reach 68%, which substantially exceeds that observed with the involvement of other target organs [6, 7]. The liver is a central metabolic and immune organ that, under septic conditions, ensures bacterial clearance and the synthesis of cytokines and acute-phase proteins. However, an excessive inflammatory response can induce pronounced hepatocyte cytolysis, leading to the development of sepsis-induced ALD [6]. ALD entails disruption of the enzymatic urea cycle, resulting in hyperammonemia, which constitutes the key pathophysiological link in the development of hyperammonemic encephalopathy (HE). The clinical manifestations of HE are nonspecific and range from subclinical disturbances to coma and lethal outcome [8]. The neurotoxic effect of ammonia on brain cells is mediated by a number of mechanisms, including glutamine-induced astrocyte swelling, oxidative stress, neuroinflammation, disruption of neurotransmitter homeostasis, and mitochondrial dysfunction [9]. In clinical practice, verification of HE is most often performed retrospectively, especially in comorbid patients with sepsis. Validated clinical and laboratory criteria are lacking; therefore, reliable identification of HE at the early stages of the pathological process is extremely challenging. Persistent hyperammonemia can induce severe cerebral damage and give rise to long-term neurological sequelae [10]. An additional factor limiting early diagnosis is the necessity of conducting a complex differential diagnosis with other cerebral lesions, which hinders timely verification of HE as the primary cause of neurological impairment. Given this diagnostic challenge, we conducted this pilot case series to describe the spectrum and evolution of MRI alterations in patients with sepsis-induced HE.

Methods

Study design and participants

This is a descriptive case series of 15 patients (10 males, 5 females; mean age 42 ± 12 years) with clinically verified sepsis and HE, in whom pathological signal changes in the brain were detected on MRI between June 2021 and February 2025. The sample size reflects the rarity of the co-occurrence of sepsis, HE, and characteristic MRI changes; all eligible patients hospitalized during the specified period were included consecutively. The diagnosis of HE was established in the presence of the following criteria: 1) confirmed sepsis (according to Sepsis-3); 2) blood ammonia level > 100 μmol/L; 3) hepatic dysfunction (ALT/AST > 2× upper limit of normal, total bilirubin > 20 μmol/L); 4) clinical signs of encephalopathy (≥ 1 point on West Haven criteria); and 5) exclusion of other causes of CNS injury (stroke, meningitis, toxic encephalopathy, etc.) based on medical history, laboratory data, and instrumental investigations. The study was approved by the Local Ethics Committee of the Regional Clinical Hospital No. 2 (Protocol No. 06/2021 dated October 3, 2021). Informed consent was obtained from all patients or their legal representatives.

Data collection

For each patient, we reviewed medical records for causes of ALD, clinical presentation, laboratory parameters (ammonia, transaminases, lactate, procalcitonin, CRP), and administered therapy.

MRI acquisition

MRI was performed in all patients within a few hours of the onset of neurological symptoms. Imaging studies were carried out using a 1.5 T scanner (Signa Voyager, General Electric). The scanning protocol comprised the following sequences: T2-weighted images (TR/TE, 3000/80 ms; slice thickness, 5 mm; interslice gap, 1.5 mm; field of view, 220×220 mm); FLAIR (TR/TE, 11 000/125 ms; slice thickness, 5 mm; interslice gap, 1.5 mm; field of view, 220×220 mm); T1-weighted images (TR/TE, 2000/10 ms; slice thickness, 5 mm; interslice gap, 1.5 mm; field of view, 220×220 mm); axial two-dimensional gradient-echo SWAN images (TR/TE, 453/14 ms; slice thickness, 5 mm; interslice gap, 1.5 mm; field of view, 220×220 mm); and diffusion-weighted imaging (DWI) with b-factors of 0 and 1000 s/mm², acquired in the axial plane using three orthogonal diffusion gradient directions with subsequent generation of isotropic maps (TR/TE, 4300/46 ms; slice thickness, 3 mm; interslice gap, 1 mm; field of view, 240×240 mm).

Image analysis

MRI data were evaluated by three experienced neuroradiologists for: lesion localization and signal characteristics on T1-WI, T2-WI/FLAIR, SWAN; DWI/ADC features (presence of diffusion restriction); and changes on follow-up. Given the descriptive nature of the study, no intergroup comparisons or statistical tests were performed.

Results

All 15 patients had ALD secondary to sepsis. Sepsis sources were urological (n = 6), surgical (n = 7), and cryptogenic (n = 2). All patients had hyperammonaemia (range 90–145 μmol/L), elevated lactate (3.2–4.8 mmol/L), transaminases (ALT 252–769 U/L; AST 175–436 U/L), total bilirubin (28–44 μmol/L), procalcitonin (2.2–18.4 ng/mL), and CRP (190–286 mg/L). Metabolic acidosis was recorded in four patients (pH 7.20–7.22). Electrolytes were unremarkable. No patient used regular medications that could explain encephalopathy. Clinical and laboratory parameters of patients with hyperammonemic encephalopathy and sepsis are presented in Table 1. All patients had decreased consciousness (GCS 3–14), and seizures occurred in 4 (26.7%).

On MRI, the most frequent pattern (13 patients, 86.7%) was symmetrical hyperintensity on T2-WI and FLAIR in the insular cortex and cingulate gyri, with restricted diffusion consistent with cytotoxic oedema (Fig. 1). One patient (6.7%) showed symmetrical basal ganglia lesions (Fig. 2), and one (6.7%) had asymmetric cortico-subcortical hemispheric lesions (Fig. 3). Diffusion restriction was present in all cases, always corresponding to the affected areas. No haemorrhagic changes were seen on SWAN.

Table 1
Main clinical and laboratory parameters of patients with hyperammonemic encephalopathy and sepsis.

Age	Sex	Source of sepsis	Ammonia levels µmol/L	ALT U/L	AST U/L	Total bilirubin µmol/L	Lactate mmol/L	Procalcitonin ng/mL	Pattern on MRI	Outcome
26	M	Urological	120	350	220	36	3,8	10,5	Insular-cingulate pattern	Regression
30	M	Urological	110	300	200	34	3,5	9,2	Insular-cingulate pattern	Regression
34	F	Urological	125	400	250	38	4,0	12,0	Insular-cingulate pattern	Regression
38	M	Urological	130	380	240	37	3,9	11,0	Insular-cingulate pattern	Regression
40	M	Urological	127	450	280	42	4,2	13,5	Insular-cingulate pattern	Regression
41	M	Urological	115	500	300	44	4,4	15,0	Insular-cingulate pattern	Regression
42	M	Surgical	125	360	230	35	3,7	10,0	Insular-cingulate pattern	Regression
42	M	Surgical	135	390	245	39	3,9	11,5	Insular-cingulate pattern	Regression
43	M	Surgical	116	420	260	40	4,1	12,5	Insular-cingulate pattern	Regression
44	M	Surgical	131	480	290	43	4,3	14,0	Insular-cingulate pattern	Regression
46	F	Surgical	100	280	190	30	3,4	8,0	Insular-cingulate pattern	Regression
50	F	Surgical	115	320	210	32	3,6	9,5	Basal ganglia lesion pattern	Regression
54	F	Surgical	118	370	235	36	3,8	10,8	Insular-cingulate pattern	Regression
58	F	Cryptogenic	105	290	195	28	3,4	7,5	Cortico-subcortical pattern	Regression
60	M	Cryptogenic	125	340	215	34	3,7	9,0	Insular-cingulate pattern	Regression

After treatment (lactulose, L-ornithine-L-aspartate, and intensive haemodialysis), all patients showed clinical improvement, normalization of liver enzymes, and reduction of ammonia. Follow-up MRI (10–14 days later) demonstrated regression of all

pathological changes (Figs. 4-6).

Discussion

Despite significant advances in intensive care, sepsis remains a high-priority global health challenge due to high mortality rates and the frequent development of multiple organ failure [11, 12]. Pathogenetically, this condition is characterized by a complex, multi-step cascade of immunological events, including a hyperinflammatory response, coagulopathy with disseminated intravascular coagulation, and pronounced hemodynamic instability [13]. In clinical practice, sepsis can initiate a wide spectrum of liver injuries, ranging from hypoxic hepatitis and septic cholestasis to secondary sclerosing cholangitis [14]. Jaundice, elevated transaminase activity, and prolonged prothrombin time serve as external markers of profound pathogenetic shifts, which are driven by a chain of systemic inflammatory events leading to hepatocyte injury.

The pathogenesis of sepsis-induced liver injury (SILI) is multicomponent and involves uncontrolled inflammation, multi-step pro-inflammatory reactions, oxidative stress, pyroptosis, and impaired autophagy [15]. Among these factors, oxidative stress acts as a key mediator that exacerbates pathophysiological processes both through direct cytolytic effects on hepatocytes and through the depletion of endogenous antioxidant defenses [16]. A logical consequence of severe hepatic dysfunction in sepsis is impaired detoxification function of the liver. The liver plays a central role in ammonia metabolism, converting it to urea in periportal hepatocytes. In SILI, ammonia elimination is critically reduced, leading to hyperammonemia (Fig. 7) [17].

Under conditions of elevated blood ammonia concentration, its penetration across the blood–brain barrier increases via diffusion of the non-ionized form (NH_3) and active transport of the ionized form (NH_4^+). This initiates a sequential series of metabolic disturbances in the central nervous system, where the leading role in detoxification shifts to astrocytes. Astrocytic glutamine synthetase catalyzes the conversion of excess ammonia and glutamate into glutamine. According to the widely accepted osmotic hypothesis, the accumulation of glutamine as an osmotically active substance causes water influx into astrocytes, their swelling, and the development of cytotoxic brain edema [18]. Moreover, a neurotransmission imbalance resulting from the downregulation of glutamate receptors against a background of excessive extrasynaptic glutamate accumulation and enhanced GABAergic inhibition contributes to the clinical manifestations of encephalopathy. This cascade of molecular events is directly reflected in MRI findings, which represent a highly valuable tool for understanding the pathophysiology of HE in vivo. In contrast to chronic liver failure, which is characterized by deposition of paramagnetic manganese in the basal ganglia, ALD associated with hyperammonemia is accompanied by selective cortical involvement of the cingulate gyrus and insula [19].

The presented results demonstrate that the combination of sepsis and ALD confers a high risk of developing HE. This finding fully supports the concept of a synergistic damaging effect of systemic inflammation and hyperammonemia on brain tissue. In the present study, among 15 patients with SILI and HE, the most frequent MRI pattern (86.7%) was symmetrical involvement of the insular cortex and cingulate gyri with cytotoxic edema. Thus, neuroimaging are of particular importance in the diagnosis of HE, among which MRI exhibits the highest sensitivity in assessing the nature and extent of injury. The selective vulnerability of the cingulate gyrus and insular cortex to ammonia is determined not by the presence of specific «ammonia receptors», but by the neurometabolic organization of these structures [20]. Key factors include the high intensity of glutamatergic neurotransmission, a marked dependence on astrocyte metabolism, and the substantial energy demands of their neuronal networks. These regions represent highly integrative cortical areas that process interoceptive, emotional, and cognitive information [21]. They are characterized by a high density of excitatory glutamatergic connections and intense synaptic activity even at rest, which renders them critically dependent on efficient astrocytic control of extracellular glutamate [21]. Moreover, the high rate of energy metabolism and reliance on mitochondrial oxidative phosphorylation make these networks exquisitely sensitive to ammonia-induced inhibition of mitochondrial enzymes, suppression of the Krebs cycle, and increased generation of reactive oxygen species, collectively leading to rapid energy deficiency [22]. Interpretation of neuroimaging findings requires careful differential diagnosis, as extensive cortical signal abnormalities can be observed in hypoxic–ischemic encephalopathy, limbic encephalitis, acute hypertensive and hyponatremic encephalopathies, posterior reversible encephalopathy syndrome, alcohol and drug intoxication, carbon monoxide or organophosphate poisoning, and Creutzfeldt–Jakob disease [23]. The key differential diagnostic criteria include: documented sepsis, the combination of two mandatory clinical components (ALD and

hyperammonemia), and characteristic neuroimaging features, namely bilateral involvement of the insular cortex and cingulate gyrus as well as a specific type (cytotoxic) of edema. A fundamental clinical feature of HE, confirmed in our study, is its potential reversibility provided that timely and aggressive correction of hyperammonemia is undertaken. Intensive hemodialysis led not only to normalization of blood ammonia, bilirubin, and transaminase levels, but also to marked regression of neurological symptoms with convincing positive dynamics on follow-up MRI examinations. This observation supports the importance of early ammonia-lowering therapy, although causality cannot be definitively established in a case series. The results of the present study further demonstrate that positive dynamics (in the form of regression of neurological symptoms and MRI changes) are expected within an interval of 10 to 14 days from the start of complex therapy, which may serve as a prognostic criterion for a favorable outcome.

Limitations

Our study has several important limitations that must be acknowledged. First, this is a descriptive case series without a control group (e.g., septic patients without HE, or non-septic hyperammonaemic patients); therefore, we cannot estimate the specificity or sensitivity of the described MRI patterns. Second, the small sample size (n = 15) limits generalizability and precludes any statistical analyses or multivariable adjustments. Third, although DWI suggested cytotoxic oedema, we did not perform quantitative ADC measurements, and the contribution of concurrent hypoperfusion or seizure-related changes cannot be entirely ruled out. Fourth, the timing of MRI and follow-up was not strictly standardized, and the reversibility was assessed qualitatively. Thus, our findings should be considered hypothesis-generating rather than confirmatory. Larger, prospective, controlled multicentre studies with serial quantitative MRI are needed to validate the diagnostic and prognostic value of the insular-cingulate pattern. Despite these limitations, this is one of the largest described series of MRI findings in sepsis-associated HE, and our observations may help clinicians recognize this condition and guide early therapy.

Conclusions

This pilot case series describes the spectrum of brain MRI abnormalities in patients with sepsis-associated hyperammonaemic encephalopathy. The bilateral insular-cingulate pattern was the most frequent finding and showed reversibility upon correction of hyperammonaemia. While MRI may provide supportive evidence for early diagnosis and therapeutic monitoring, particularly when the insular-cingulate pattern is observed in the appropriate clinical context. Controlled studies with larger cohorts are essential to determine the diagnostic accuracy and clinical utility of these neuroimaging features. Nonetheless, early recognition of sepsis-induced liver dysfunction and prompt ammonia-lowering therapy remain the cornerstones of improving outcomes in this patient population.

Abbreviations

ALD
Acute liver dysfunction
ADC
Apparent diffusion coefficient
CNS
Central nervous system
DWI
Diffusion-weighted imaging
GCS
Glasgow Coma Scale
HE
Hyperammonemic encephalopathy
MRI
Magnetic resonance imaging
SILI

Sepsis-induced liver injury
WI
Weighted images

Declarations

Ethics approval and consent to participate

This study was reviewed and approved by the Local Ethics Committee of (Approval No.). The study was conducted in accordance with the Declaration of Helsinki. Written informed consent was obtained from all participants prior to their inclusion in the study.

Consent for publication

The consent for publication has been obtained from all participants.

Competing interests

The authors declare no competing interests.

Funding

Author Contribution

Conceptualisation and writing of the original draft were conducted by RT. Case selection and investigation of the clinical data was conducted by RT. Review of the H&E slides was conducted by TT. Reviewing and editing the manuscript was conducted by TT, and RT. TK confirm the authenticity of all the raw data. YS participated in the preparation and analysis of the radiological images. All authors reviewed the manuscript. All authors contributed to the manuscript writing.

Acknowledgements

The authors thank the study participants for their participation in this study.

References

1. Singer M, Deutschman CS, Seymour CW, Shankar-Hari M, Annane D, Bauer M, Bellomo R, Bernard GR, Chiche JD, Coopersmith CM, Hotchkiss RS, Levy MM, Marshall JC, Martin GS, Opal SM, Rubenfeld GD, van der Poll T, Vincent JL, Angus DC (2016) The Third International Consensus Definitions for Sepsis and Septic Shock (Sepsis-3). JAMA 315(8):801–810. 10.1001/jama.2016.0287
2. Qin C, Ma D, Pang L, Hu M, Lin S, Zhou Z, Xu X, Ji C (2025) Prognostic factors of sepsis: a systematic review and meta-analysis. BMC Infect Dis 25(1):1670. 10.1186/s12879-025-12094-9
3. Jalal SM, Jalal SH, Alabdullatif AA, Alasmakh KE, Alnasser ZH, Alhamdan WY (2025) Evaluating Sepsis Management and Patient Outcomes: A Comprehensive Retrospective Study of Clinical and Treatment Data. J Clin Med 14(10):3555. 10.3390/jcm14103555
4. Liu Y, Wei Z, Liu W, Hao H, Ba T, Zhang S, Bao B, Li C, Kong L, Zhang F (2025) Sepsis related multi-organ dysfunction: a global perspective on lung and gastrointestinal mortality and management framework. BMC Infect Dis 26(1):142. 10.1186/s12879-025-12062-3
5. Srdić T, Đurašević S, Lakić I, Ružičić A, Vujović P, Jevđović T, Dakić T, Đorđević J, Tosti T, Glumac S, Todorović Z (2024) Jasnić N. From Molecular Mechanisms to Clinical Therapy: Understanding Sepsis-Induced Multiple Organ Dysfunction. Int

J Mol Sci 25(14):7770. 10.3390/ijms25147770

6. Xu X, Yang T, An J, Li B, Dou Z (2025) Liver injury in sepsis: manifestations, mechanisms and emerging therapeutic strategies. Front Immunol 16:1575554. 10.3389/fimmu.2025.1575554
7. Guo Y, Guo W, Chen H, Sun J, Yin Y (2025) Mechanisms of sepsis-induced acute liver injury: a comprehensive review. Front Cell Infect Microbiol 15:1504223. 10.3389/fcimb.2025.1504223
8. Ciselle Meier K, Burns C, Manolikos D, Fatovich DA, Bell (2024) Hyperammonaemia: review of the pathophysiology, aetiology and investigation. Pathology,56. 6763–772. doi.org/10.1016/j.pathol.2024.06.002
9. Zhao L, Hou S, Na R et al (2022) Prognostic role of serum ammonia in patients with sepsis-associated encephalopathy without hepatic failure. Front Public Health 10. 10.3389/fpubh.2022.1016931.1016931
10. Denk CH, Kunzmann J, Maieron A, Wöhrer A, Quinot V, Oberndorfer S (2024) Histopathological examination of characteristic brain MRI findings in acute hyperammonemic encephalopathy: A case report and review of the literature. Neuroradiol J 37(5):630–635. 10.1177/19714009231212370
11. Gomanova LI, Brazhnikov AY (2021) Sepsis in the XXI Century: Etiology, Risk Factors, Epidemiological Features, Complications, Prevention. Epidemiol Vaccinal Prev 20(3):107–117 (In Russ.). 10.31631/2073-3046-2021-20-3-107-117
12. Malkov PG, Frank GA (2025) Sepsis: A Brief Overview of the Key Concepts. 21(3):51–56. 10.15360/1813-9779-2025-3-2566
13. Srdić T, Đurašević S, Lakić I, Ružičić A, Vujović P, Jevđović T, Dakić T, Đorđević J, Tosti T, Glumac S, Todorović Z (2024) Jasnić N. From Molecular Mechanisms to Clinical Therapy: Understanding Sepsis-Induced Multiple Organ Dysfunction. Int J Mol Sci 25(14):7770. 10.3390/ijms25147770
14. Lu Y, Shi Y, Wu Q, Sun X, Zhang WZ, Xu XL, Chen W (2023) An Overview of Drug Delivery Nanosystems for Sepsis-Related Liver Injury Treatment. Int J Nanomed 18:765–779. 10.2147/IJN.S394802
15. Chen JW, Liu CY, Li S, Wu SW, Cai C, Lu MQ (2024) Sepsis-associated liver injury: Mechanisms and potential therapeutic targets. World J Gastroenterol 30(42):4518–4522. 10.3748/wjg.v30.i42.4518
16. Xu X, Yang T, An J, Li B, Dou Z (2025) Liver injury in sepsis: Manifestations, mechanisms and emerging therapeutic strategies. Front Immunol 16:1575554. 10.3389/fimmu.2025.1575554
17. Zhao L, Hou S, Na R et al (2022) Prognostic role of serum ammonia in patients with sepsis-associated encephalopathy without hepatic failure. Front Public Health 10. 10.3389/fpubh.2022.1016931.1016931
18. Wang P, Yan J, Shi Q, Yang F, Li X, Shen Y, Liu H, Xie K, Zhao L (2023) Relationship between Nonhepatic Serum Ammonia Levels and Sepsis-Associated Encephalopathy: A Retrospective Cohort Study. Emerg Med Int 2023:6676033. 10.1155/2023/6676033
19. Kerbert AJC, Engelmann C, Habtesion A, Kumar P, Hassan M, Qi T, Volkert I, Otto T, Hall A, Khetan VU, Olde Damink S, Aguilar F, Chollet C, Brunet L, Clària J, Moreau R, Arroyo V, Coenraad MJ, Mehta G, Castelli F, Trautwein C, Fenaille F, Andreola F, Jalan R (2025) Hyperammonemia induces programmed liver cell death. Sci Adv 11(10):eado1648. 10.1126/sciadv.ado1648
20. Denk CH, Kunzmann J, Maieron A, Wöhrer A, Quinot V, Oberndorfer S (2024) Histopathological examination of characteristic brain MRI findings in acute hyperammonemic encephalopathy: A case report and review of the literature. Neuroradiol J 37(5):630–635. 10.1177/19714009231212370
21. Luciano Simone F, Caruana E, Borra SD, Sorbo A, Jezzini S, Rozzi G, Luppino M, Gerbella (2025) Anatomo-functional organization of insular networks: From sensory integration to behavioral control. Progress in Neurobiology. 247. doi.org/10.1016/j.pneurobio.2025.102748
22. Bakharji A, Alarfaj H, Omar S, Alzahrani S, Alzahrani N, Alahmari F, Al Mulhim S, Almuhaish H, Bashir S, Al-Harbi TM (2025) Brain magnetic resonance imaging findings in hyperammonemic hepatic encephalopathy: A case series and literature review. Biomed Rep 22(6):98. 10.3892/br.2025.1976
23. Wakrim S, El Mekkaoui A, Benlenda O, Nainia K, Nassik H (2022) Brain MR imaging in acute hyperammonemic: Case report. Radiol Case Rep 17(10):4046–4048. 10.1016/j.radcr.2022.07.060

Figures

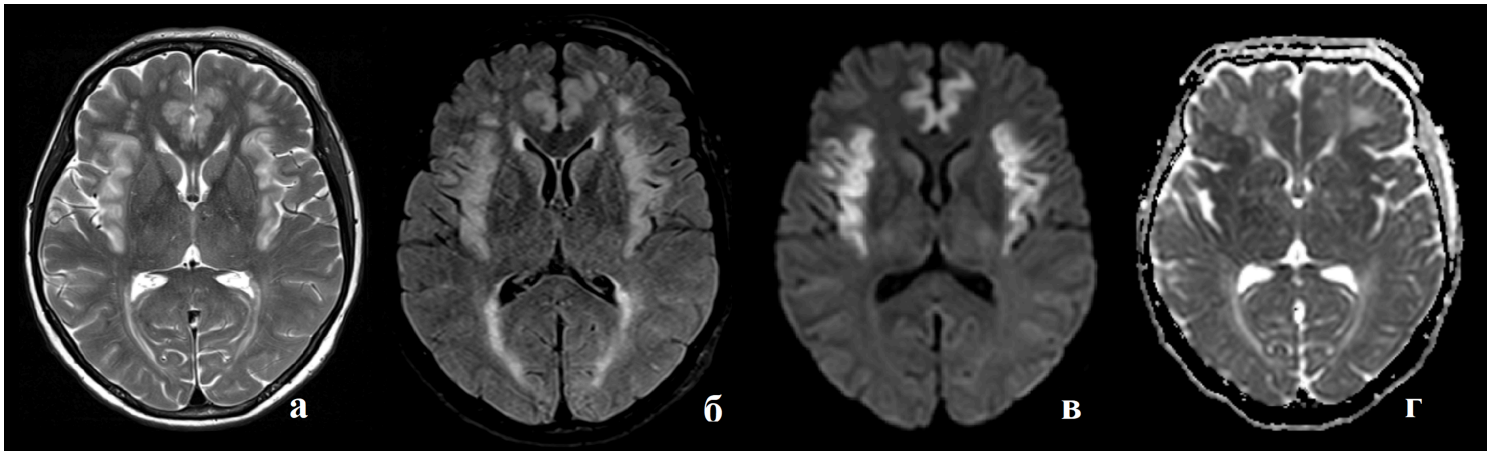


Figure 1

Brain MRI of Patient 1 with Hyperammonemic Encephalopathy and Abdominal Sepsis: (a) T2-weighted imaging; (b) T2-FLAIR; (c) DWI; (d) ADC. Bilateral symmetrical areas of abnormal signal intensity are observed in the insular cortex and cingulate gyrus with diffusion restriction.

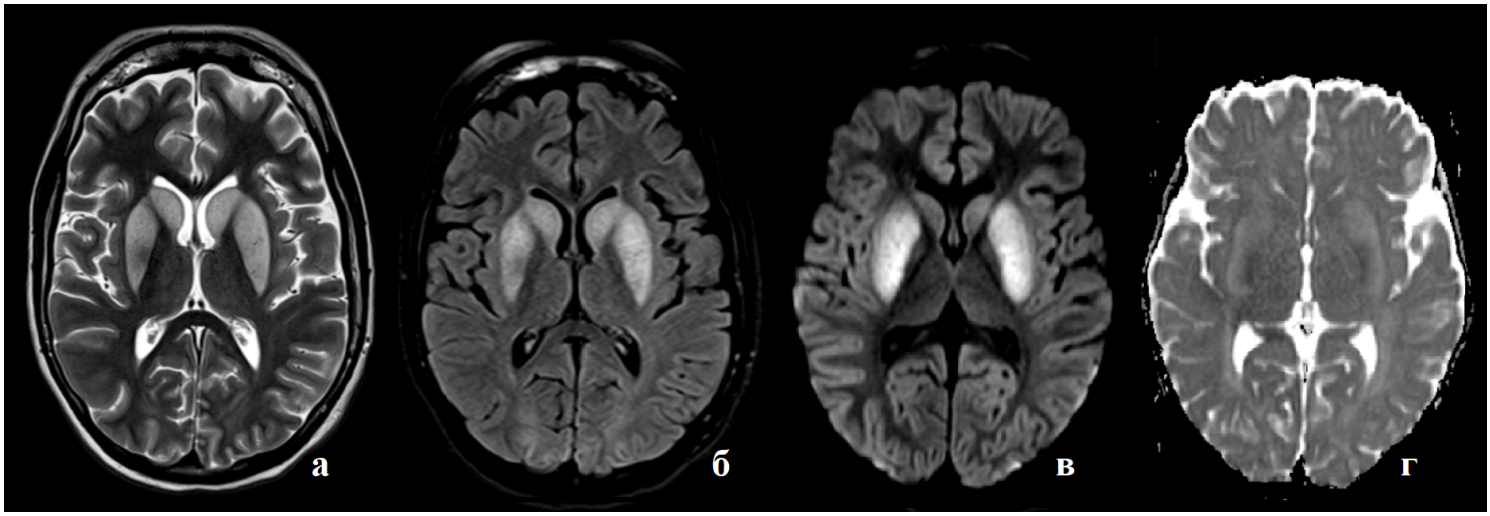


Figure 2

Brain MRI of Patient 2 with Hyperammonemic Encephalopathy and Abdominal Sepsis: (a) T2-weighted imaging; (b) T2-FLAIR; (c) DWI; (d) ADC. Symmetrical bilateral lesions of basal ganglia with moderate diffusion restriction.

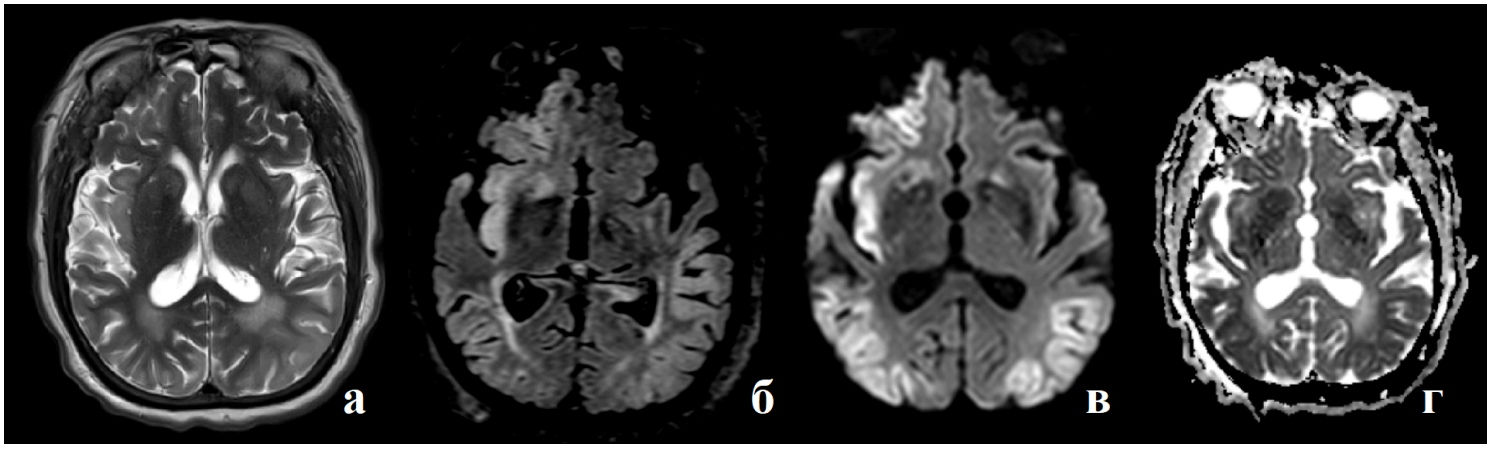


Figure 3

Brain MRI of Patient 3 with Hyperammonemic Encephalopathy and Cryptogenic Sepsis: (a) T2-weighted imaging; (b) T2-FLAIR; (c) DWI; (d) ADC. Bilateral, asymmetric involvement of the cortical structures of the temporal and occipital lobes, as well as the insular cortex, characterized by restricted diffusion.

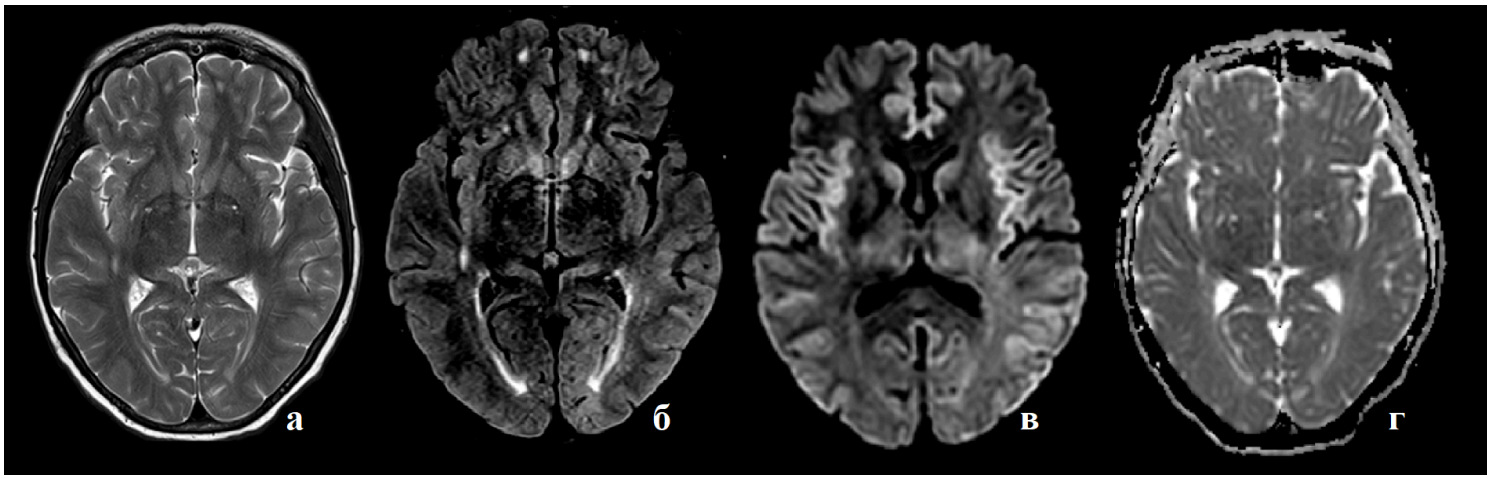


Figure 4

Follow-up brain MRI of Patient 1 performed 10 days after the corrected therapy: (a) T2-weighted imaging; (b) T2-FLAIR; (c) DWI; (d) ADC. A marked regression of cytotoxic edema is observed in the insular cortex and cingulate gyri, with residual mild vasogenic edema involving the cortex.

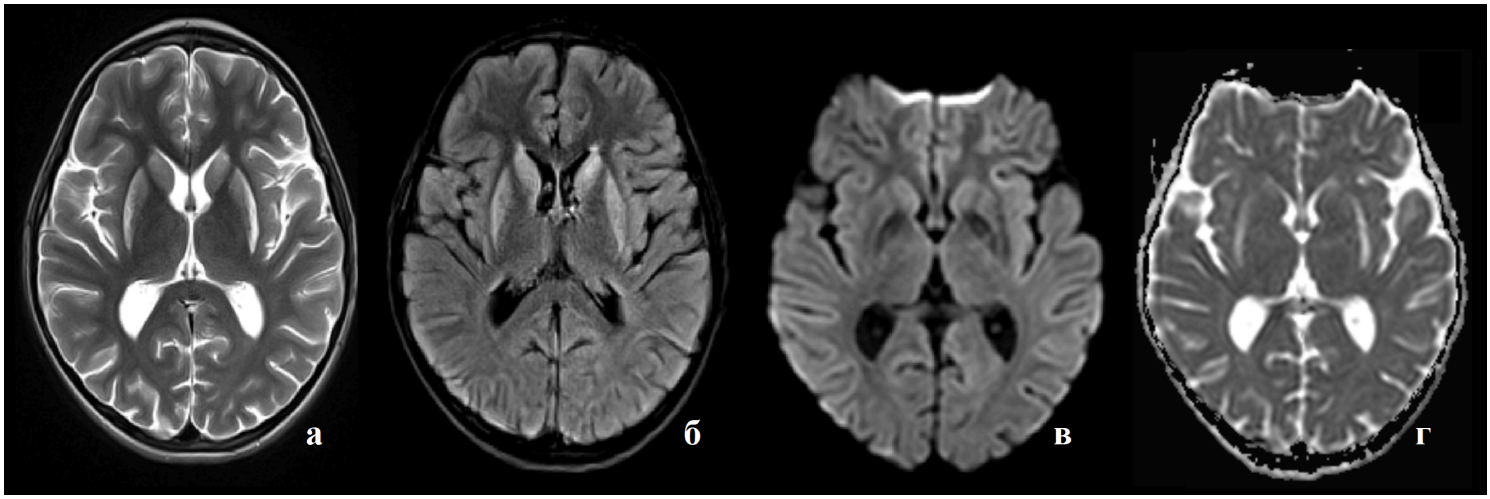


Figure 5

Follow-up brain MRI of Patient 2 performed 12 days after the corrected therapy: (a) T2-weighted imaging; (b) T2-FLAIR; (c) DWI; (d) ADC. A marked regression of cytotoxic edema is observed in the bilateral basal ganglia region.

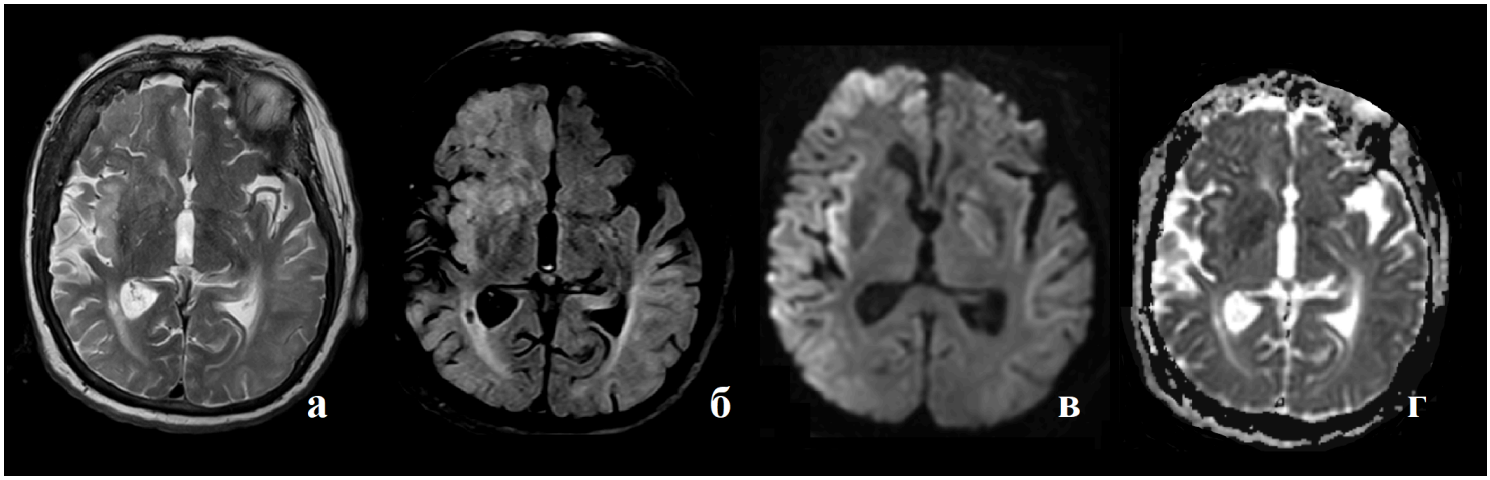


Figure 6

Follow-up brain MRI of Patient 3 performed 14 days after the corrected therapy: (a) T2-weighted imaging; (b) T2-FLAIR; (c) DWI; (d) ADC. In the cortical and subcortical areas of the frontal, temporal, insular and occipital lobes, a pronounced regression of cytotoxic changes is observed.

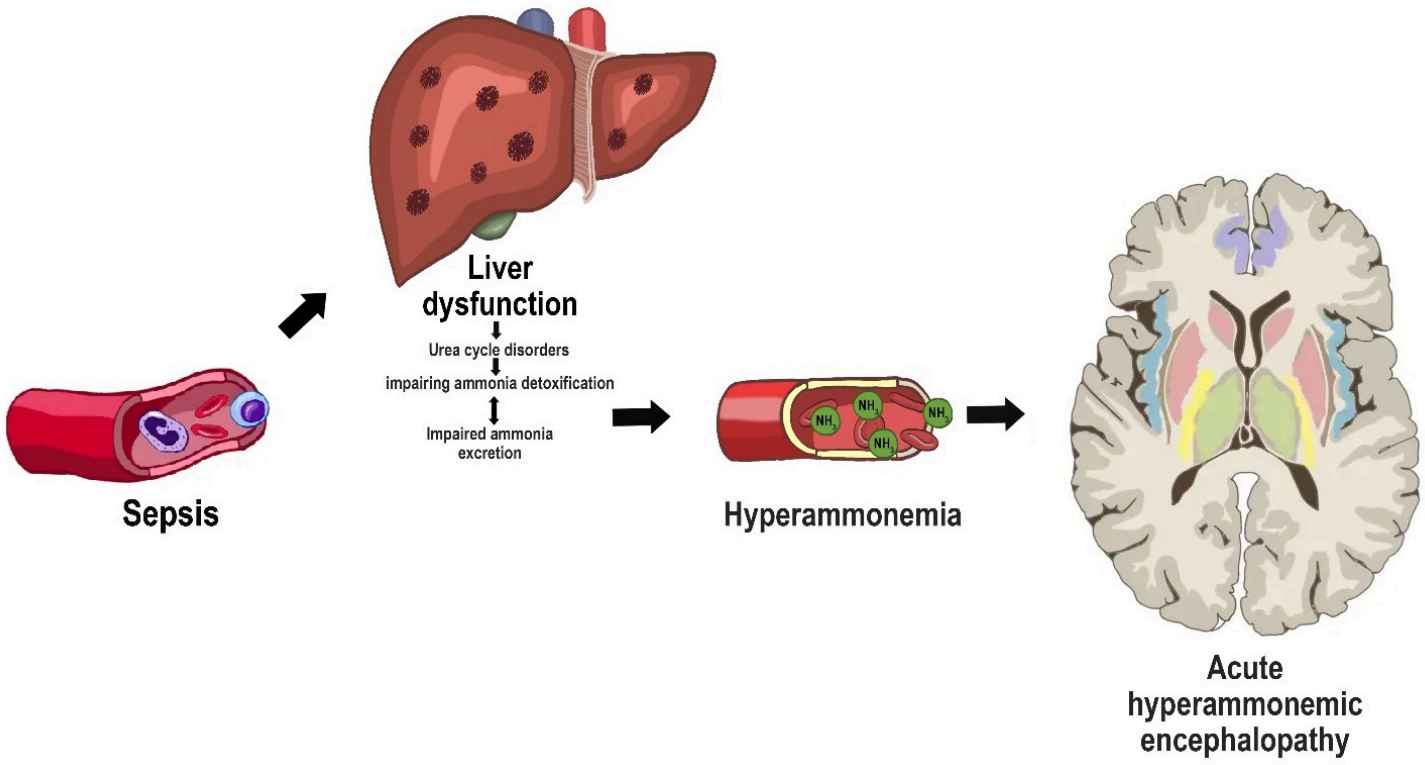


Figure 7

Pathogenetic mechanisms of development of hyperammonemic encephalopathy in sepsis